Corrosion Inhibition Potentiality of 5-Nitro-1H-Benzimidazol-2(3H)-One Derivatives for Mild Steel in Hydrochloric Acid: Electrochemical and Weight Loss Studies

Bouayad K[1,2*], Kandri Rodi Y[1], Elmsellem H[3], El-Ghadraoui EH[2], Kadmi Y[6,7,8,9*], Ouzidan Y[1], Sebbar NK[4], Steli H[10], Essassi EM[4,5], Hammouti B[2]

[1]*Laboratoire de Chimie Organique Appliquée, Université Sidi Mohamed Ben Abdallah, Faculté des Sciences et Techniques, Route d'Immouzzer, BP 2202, Fès, Morocco*

[2]*Laboratoire de Chimie de la matière condensée, Faculté des Sciences et Techniques Université Sidi Mohamed Ben Abdallah, Fès, Morocco*

[3]*Laboratoire de chimie analytique appliquée, matériaux et Environment (LC2AME), Faculté des Sciences, B.P. 717, 60000 Oujda, Morocco*

[4]*Laboratoire de Chimie Organique Hétérocyclique, URAC 21, Pôle de Compétences Pharmacochimie, Mohammed V University in Rabat, Faculté des Sciences, Av. Ibn Battouta, BP 1014 Rabat, Morocco*

[5]*Moroccan Foundation for Advanced Science, Innovation, and Research (MASCIR), Rabat Design Center, Rue Mohamed Al-Jazouli, Madinat El Irfane, Rabat, Morocco*

[6]*Université d'Artois, EA 7394, Institute Charles Viollette, Lens, F-62300, France*

[7]*ISA Lille, EA 7394, Institute Charles Viollette, Lille, F-59000, France*

[8]*Ulco, EA 7394, Institute Charles Viollette, Boulogne sur Mer, F-62200, France*

[9]*Université de Lille, EA 7394, Institut Charles Viollette, Lille, F-59000, France*

[10]*Laboratoire mécanique & énergétique, Faculté des Sciences, Université Mohammed Premier, Oujda, Morocco*

*****Corresponding author:** Kadm Yi, Université d'Artois, EA 7394, Institut Charles Viollette, Lens, F-62300, France, E-mail: yassine.kadmi@gmail.com*

ABSTRACT

The adsorption and inhibition effects of 5-nitro-1H-benzimidazol-2(3H)-one (P2) on mild steel corrosion in 1 M HCl have been studied by electrochemical and weight loss methods. Results obtained showed that inhibition efficiency increases with concentration and maximum value was obtained at 10^{-3} M concentration. From the results, it is concluded that compound P2 inhibited mild steel corrosion in 1 M HCl by adsorbing on the metal surface. Polarization results showed that P2 act as mixed type inhibitor. The adsorption of P2 onto the mild steel surface was described by the Langmuir adsorption isotherm.

Keywords: Corrosion inhibition, Mild steel, EIS, Weight loss, 5-nitro-1H-benzimidazol-2(3H)-one.

INTRODUCTION

The application of inhibitors is used to reduce the metal dissolution and iron build up in the pickling baths, because the corrosion protection of mild steel is a significant concern among the corrosion scientist and material technologist. Although, mild steel has remarkable economic and substantial applications, its deprived corrosion resistance in acids limits the usage. Acid solutions are essentially used in metal finishing industries, acidizing of oil wells, cleaning of boilers and heat exchangers [1-4]. The most effective and efficient inhibitors are organic compounds containing heteroatom (O, N, S and P) and having p bonds in their structures. The efficiency of an inhibitor is largely dependent on its adsorption on the metal surface. The adsorption of these molecules depends mainly on certain Physico-chemical properties of the inhibitor molecule such as functional groups, steric factors, aromaticity, electron density at the donor atoms and π orbital character of donating electrons [5,6] and the electronic structure of the molecules [7,8]. Benzimidazole derivatives have occupied a prominent place in medicinal chemistry because of their significant properties as therapeutics in clinical applications. Benzimidazole is a versatile pharmacophore producing a diverse range of biological activities including antimicrobial [9-11], anti-inflammatory [12], anthelmintic [13] and antiviral [14-16] properties.

The title compound (P2) was obtained in good yield by the condensation of 3-nitro-1,2-phenylenediamine with ethyl chloroformate. The aim of the present study is to evaluate the corrosion inhibition efficiency of mild steel corrosion in 1 M HCl of 5-nitro-1H-benzoimidazol-2(3H)-one (P2) (Figure 1). The structure of the product obtained is determined by spectroscopic and elemental analysis. Regarding the adsorption of inhibitor on the metal surface, two types of interactions are responsible. One is physical adsorption, which involves electrostatic forces between ionic charges or dipoles of the adsorbed species and the electric charge at the metal/solution interface. The other is chemical adsorption, which involves charge sharing or charge transfer from inhibitor molecules to the metal surface to form coordinate type of bond [17,18].
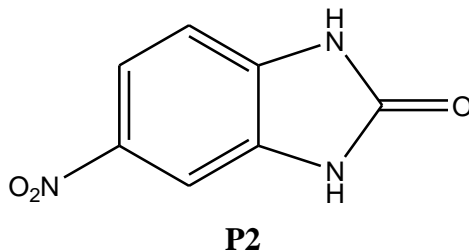
Figure 1: Chemical structure of 5-nitro-1H-benzimidazol-2(3H)-one (P2).

Theoretical calculations have been used recently to explain the mechanism of corrosion inhibition, which proved to be a very powerful tool in this direction [19-21]. The geometry of inhibitor molecule in its ground state, nature of its molecular orbitals, HOMO (highest occupied molecular orbital) and LUMO (lowest unoccupied molecular orbital) are directly involved in the corrosion inhibition activity.

EXPERIMENTAL PROCEDURES

Specimens and solutions preparation

Mass loss tests were carried out on mild steel specimen of chemical composition: C-0.05%, Mn-0.6%, P- 0.36%, Si-0.03% and the remainder iron. Mild steel specimens were used in the sheet form of 1.5 cm × 1.5 cm × 0.5 cm dimensions. Before mass loss test, mild steel specimens were cleaned with acetone, dried and stored moisture free desiccators. The aggressive solutions of 1.0 M HCl were prepared by dilution of analytical grade 37% HCl with distilled water. The concentration range of P2 employed was $10^{-6}M – 10^{-3}M$ in 1M HCl solutions.

Synthesis of inhibitor

To a solution of (0.212 mmole) of 3-nitro-1,2-phenylenediamine in 50 ml of pyridine was added 2.43 ml (0.255 mmole) of ethyl chloroformate. The magnetic stirring was maintained at 0°C for 15 minutes. Then, the reaction mixture is refluxed for 24 hours. After evaporation of pyridine, the residue obtained was washed with ethanol and then filtered.
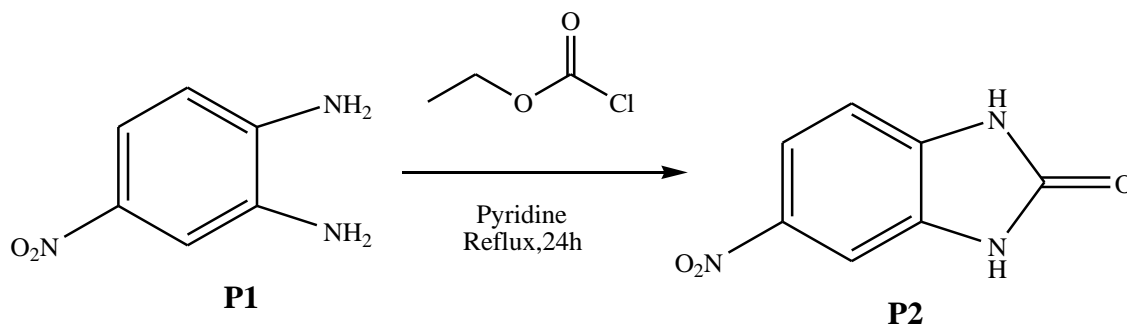
Scheme 1: Synthesis of 5-nitro-1H-benzimidazol-2(3H)-one (P2).

The analytical and spectroscopic data are conforming to the structure of compound formed:

(P2): Yield: 78%; M.p >270°C; NMR1H (DMSO-d6) δ ppm: 11.35(s, 1H, NH); 11.11(s, 1H, NH); 7.84(dd, 1H, HAr, J1=1.85 Hz, J2=8.58Hz); 7.63(d, 1H, Har, J=1.33Hz); 7.02(d, 1H, HAr, J=8.61Hz). NMR13C (DMSO-d6) δ ppm:155.90(C=O); 141.61, 136.05, 130.08(Cq); 118.07,108.35, 104.02(CHAr).

178

Mass loss method

Mass loss is one of the easiest and widely used techniques of preliminary inhibition assessment. The pre-weighed and polished mild steel sheet was immersed in 100 ml of 1M HCl solution without and with various concentrations of P2 for 6 hrs at 308K.

After 6 hrs, the sheet was taken from the solution, washed with double distilled water, rinsed with acetone, dried and reweighed. The mass of each steel sheet was measured before and after immersion using an analytical balance. Tests were done in triplicate at the same time, and the average mass loss was calculated.

Electrochemical measurements

Electrochemical measurements, including stationary methods and transient (EIS) were performed in a three-electrode cell. Pure mild steel specimen was used as the working electrode; saturated calomel (SCE) as reference electrode and an area platinum as counter electrode (CE) were used. All potentials were measured against CE. The working electrode was immersed in a test solution for 30 min until the corrosion potential of the equilibrium state (E_{corr}) was achieved using a type PGZ100 potentiostat. The potentio-dynamic polarization curves were determined by a constant sweep rate of 1 mv/s. The measurements of the transitory method (EIS) were determined; using ac signals of amplitude 10 mV peak to peak at different conditions in the frequency range of 100 kHz to 10 mHz.

Quantum chemical calculations

Quantum chemical calculations are used to correlate experimental data for inhibitors obtained from different techniques (viz., electrochemical and weight loss) and their structural and electronic properties. According to Koopman's theorem [22], E_{HOMO} and E_{LUMO} of the inhibitor molecule are related to the ionization potential (I) and the electron affinity (A), respectively. The ionization potential and the electron affinity are defined as $I = -E_{HOMO}$ and $A = -E_{LUMO}$, respectively. Then absolute electronegativity (χ) and global hardness (η) of the inhibitor molecule are approximated as follows [23]:

$$x = \frac{1+A}{2}, \quad x = -\frac{1}{2}\left(E_{HOMO} + E_{LUMO}\right) \qquad (1)$$

$$\eta = \frac{1-A}{2}, \quad \eta = -\frac{1}{2}\left(E_{HOMO} - E_{LUMO}\right) \qquad (2)$$

Where $I = -E_{HOMO}$ and $A = -E_{LUMO}$ are the ionization potential and electron affinity respectively.

The fraction of transferred electrons ∆N was calculated according to Pearson theory [24]. This parameter evaluates the electronic flow in a reaction of two systems with different electronegativity's, in particular case; a metallic surface (Fe) and an inhibitor molecule. ∆N is given as follows:

$$\Box N = \frac{xFe - xinh}{2\left(\eta Fe + \eta inh\right)} \text{s} \qquad (3)$$

Where χFeand χinh denote the absolute electronegativity of an iron atom (Fe) and the inhibitor molecule, respectively; ηFe and ηinh denote the absolute hardness of Fe atom and the inhibitor molecule, respectively. In order to apply the eq. 6 in the present study, a theoretical value for the electronegativity of bulk iron was used χFe = 7 eV and a global hardness of ηFe = 0, by assuming that for a metallic bulk I = A because they are softer than the neutral metallic atoms [24].

The electrophilicity has been introduced by Sastri et al. [25], is a descriptor of reactivity that allows a quantitative classification of the global electrophilic nature of a compound within a relative scale. They have proposed the ω as a measure of energy lowering owing to maximal electron flow between donor and acceptor and ω is defined as follows.

$$\omega = \frac{x^2}{2\eta} \qquad (4)$$

The Softness σ is defined as the inverse of the η [26]

$$\sigma = \frac{1}{\eta} \text{ s} \qquad (5)$$

RESULTS AND DISCUSSION

Weight loss study

Weight loss measurements were carried out in 1 M HCl in the absence and presence of different concentrations of P2 at 308 K after 6 h immersion period. Table 1 presents the corrosion rate, inhibition efficiency (Ew%) for P2 at different concentrations. The results show that this compound inhibits the corrosion of mild steel in 1M HCl solutions given that the corrosion rate was reduced in the presence of the P2 compared to the HCl solution. The corrosion rate was found to depend on the concentration of the P2. Inspection of the table revealed a decrease in corrosion rate as the concentration of the P2 increased. It could be also observed from the Table 1 that inhibition efficiency increased with increase in the concentration of the P2. It is noted that the maximum inhibition efficiency obtained for P2, is 91% at 308 K with the highest concentration (10−3M) of the inhibitor studied. The inhibition behavior of this P2 for mild steel corrosion in the acidic medium can be attributed to the adsorption of the components on the mild steel surface, which retards the dissolution of the metal by blocking its active corrosion sites [27-29]. Consequently, the corrosion rate is reduced and the inhibition efficiency is increased as the P2 concentration is increased.

Table 1: Weight loss measurements of different concentration with and without presence of (P2).

Inhibitor	Concentration (M)	Corrosion rate (mg/cm².h)	Efficiencies %
1M HCl	-	0.8200	-
Inhibitor (P2)	10^{-6}	0.41	50
	10^{-5}	0.3	63
	10^{-4}	0.21	74
	10^{-3}	0.07	91

Adsorption isotherm

Basic information on the interaction between the inhibitor and the mild steel surface can be provided by the adsorption isotherm. In order to obtain the isotherm, the linear relation between degree of surface coverage (θ) values and inhibitor concentration (Cinh) must be found. Attempts were made to fit the θ values to various isotherms including Langmuir, Temkin, Frumkin and Flory–Huggins. The best linear relationship was attained using Langmuir adsorption isotherm. This model has also been used for other inhibitor systems [30,31]. According to this adsorption isotherm, θ is related to the inhibitor concentration, C, and adsorption equilibrium constant, Kads, through the following expression:

$$\frac{C}{\theta} \quad = \quad \frac{1}{k} + C \qquad\qquad (6)$$

The plot of C/θ versus C gave straight lines (Figure 2) with regression close to unity confirming that the adsorption of (P2) on mild steel surface in 1M HCl medium obeys the Langmuir adsorption isotherm. The free energy of adsorption was calculated using the following relations:

$$K = \frac{1}{55.55} \exp\left(\frac{\Delta G^0_{ads}}{RT}\right) \qquad\qquad (7)$$

Where R is the universal gas constant, T is the absolute temperature, Kads is the equilibrium constant for adsorption process, and 55.5 is the molar concentration of water in solution (mol L^{-1}).
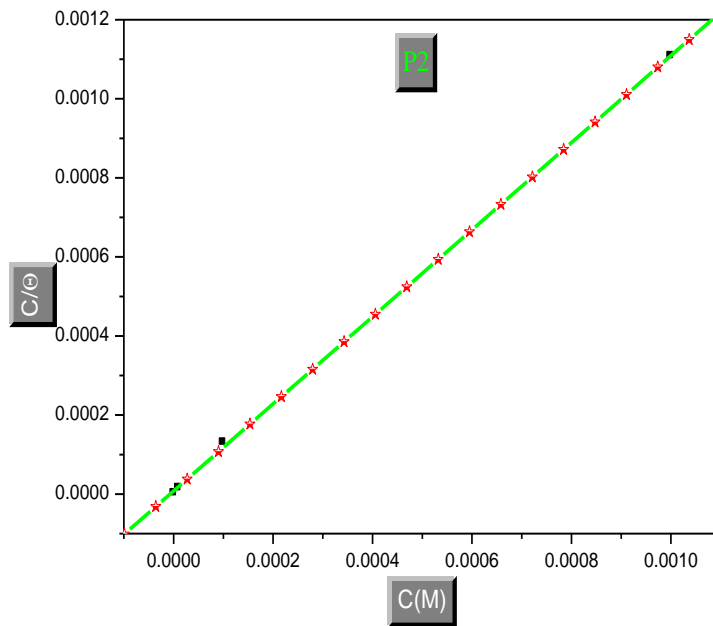

Figure 2: Langmuir isotherm plots for the adsorption of inhibitor on mild steel.

Table 2: The calculated value of K_{ads} and ΔG°_{ads} for mild steel in 1 M HCl containing compound (P2) at 308 K.

Inhibitor	Slope	R^2	K_{ads} (M^{-1})	ΔG°_{ads} (kJ mol^{-1})
P1	1.10242	0.999	1.32 10^5	-40.44

The calculated parameters are reported in the Table 2. Negative values of the $\Delta G°ads$ reflect spontaneous adsorption and strong interaction of inhibitory molecules on the surface of the mild steel. In general, values of around or below $\Delta G°ads$ -20 kJ.mol^{-1} are compatible with physical-sorption and those around or more negative than -40 kJ.mol^{-1} involve chemi-sorptions [32].
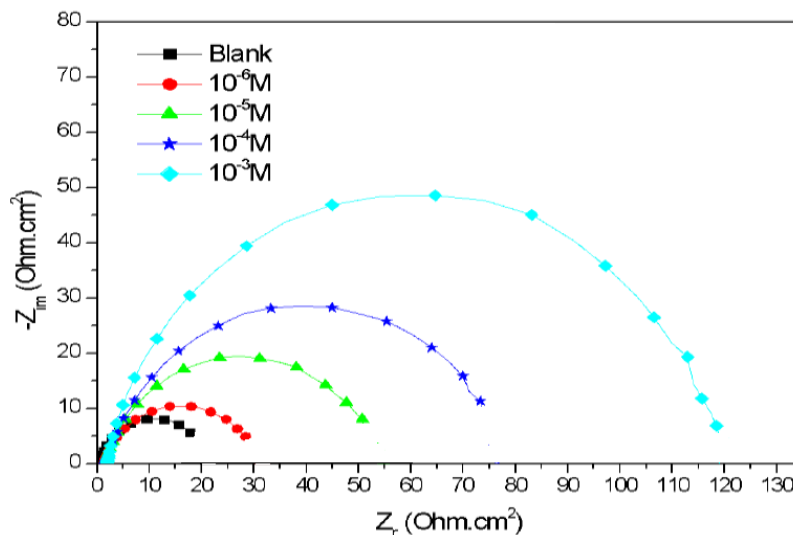
EIS study

Figure 3: Nyquist curves for mild steel in 1 M HCl for selected concentrations of P2 at 308 K.

The impedance spectra were analyzed by fitting to the equivalent circuit model shown in Figure 3, which has been used previously to adequately model the mild steel/acid interface [33,34], where Rs is the solution resistance, Rct denotes the charge-transfer resistance and CPE is constant phase element. The introduction of CPE into the circuit was necessitated to explain the depression of the capacitance semicircle, which corresponds to surface heterogeneity resulting from surface roughness, impurities, and adsorption of inhibitors [35,36]. The impedance of this element is frequency-dependent and can be calculated using the Eq. (8):

$$Z_{CPE} = \frac{1}{Q(j\omega)^n} \qquad \textbf{(8)}$$

where Q is the CPE constant (in Ω^{-1} Sn cm^{-2}), ω is the angular frequency (in rad s−1), j2 = -1 is the imaginary number and n is a CPE exponent which can be used as a gauge for the heterogeneity or roughness of the surface [37,38]. In addition, the double layer capacitances, Cdl, for a circuit including a CPE were calculated by using the following Eq. (9):

$$C_{dl} = (Q.R_{ct}^{1-n})^{1/n} \qquad \textbf{(9)}$$

The fitted parameters along with percentage inhibition efficiencies, (E%) EIS are tabulated in Table 3. For all the inhibitors, diameter of the capacitive loop is seen to increase gradually with concentration, which is manifested in progressively increasing Rct values with concomitant decrease in values of the double layer capacitance, Cdl. This suggests that the extent of adsorption increases with concentration of the inhibitors and thereby provides better barrier towards charge transfer reactions at the metal–solution interface [39].

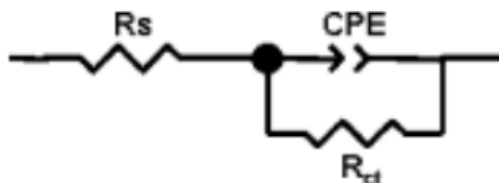**Figure 4:** Equivalent electrical circuit corresponding to the corrosion process on the mild steel in HCl.

Table 3: AC-impedance parameters for corrosion of mild steel for selected concentrations of P2 in 1 M HCl at 308 K.

Blank	Conc (M)	R_s (Ωcm^2)	R_{ct} t(Ωcm^2)	10-4 Q ($\Omega^{-1} cm^2 S^{-n}$)	n	Cdl ($\mu F cm^{-2}$)	E (%)
	1M	0.54	20	4.65	0.89	149	-
	10^{-6}	1.34	29	3.09	0.82	101	32
P2	10^{-5}	1.51	52	2.42	0.83	82	61
	10^{-4}	1.58	74	1.67	0.82	52	73
	10^{-3}	1.92	116	0.87	0.80	39	83

Potentio-dynamic polarization curves

The potentiodynamic polarization curves for mild steel in HCl 1M solution in the absence and presence of different concentrations of this inhibitor are shown in Figure 5 at 308 K. It is apparent from the Figure 5, that the nature of the polarization curves remains the same in the absence and presence of inhibitor but the curves shifted towards lower current density in the presence of inhibitor, indicating that the inhibitor molecules retard the corrosion process.

The corrosion current densities and corrosion potentials were calculated by extrapolation of the linear parts of anodic and cathodic curves to the point of intersection.
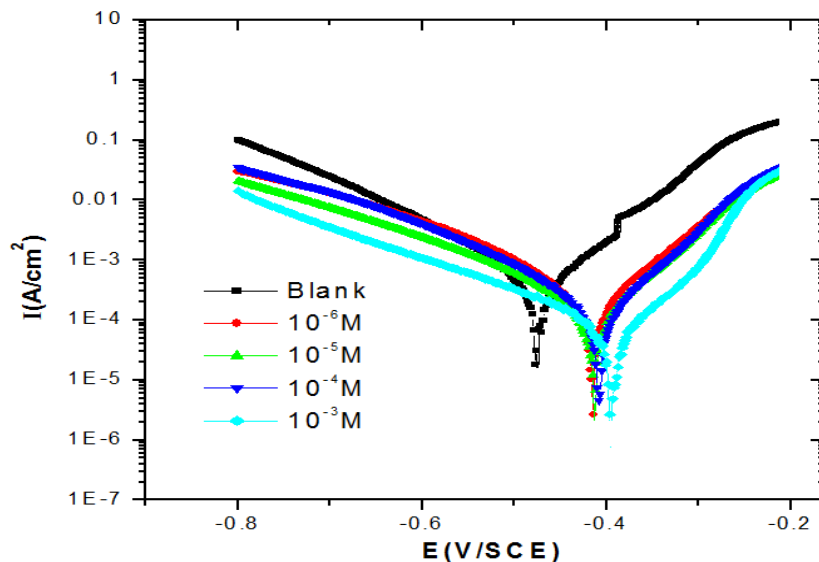
Figure 5: Polarization curves of mild steel in HCl 1M containing different concentrations of (P2) at 308 K.

Table 4: Polarization parameters and the corresponding inhibition efficiency for the corrosion of mild steel in HCl1M containing different concentrations of (P2) at 308 K.

C (M)	$-E_{corr}$ (mV_{SCE})	I_{corr} ($\mu A.cm^{-2}$)	β_a ($mV.dec^{-1}$)	$-\beta_c$ ($mV.dec^{-1}$)	E_p (%)
Blank	475	1205	98	186	--
10^{-6}	409	579	79	154	52
10^{-5}	407	294	72	137	76
10^{-4}	402	167	81	149	86
10^{-3}	400	103	67	172	91

The results revealed that increasing the concentration of inhibitor leads to a decrease in corrosion current densities and an increase in inhibition efficiency (Ep%), suggesting the adsorption of inhibitor molecules at the surface of mild steel to form a protective film on the steel surface [40,41]. The presence of P2 causes a minor change in E_{corr} values with respect to the E_{corr} value in the absence of P2. This implies that the inhibitor act as a mixed-type inhibitor, affecting both anodic and cathodic reactions [42].

The maximum displacement in our study is 75 mV, which indicates that this inhibitor act as a mixed-type. If the displacement in E_{corr} is more than $\pm 85mV$ relating to the corrosion potential of the blank, the inhibitor can be considered as a cathodic or anodic type [43]. If the change in E_{corr} is less than ± 85 mV, the corrosion inhibitor may be regarded as a mixed type.

Computational theoretical studies

The FMOs (HOMO and LUMO) are very important for describing chemical reactivity. The HOMO containing electrons, represents the ability (EHOMO) to donate an electron, whereas, LUMO haven't not electrons, as an electron acceptor represents the ability (ELUMO) to obtain an electron. The energy gap between HOMO and LUMO determines the kinetic stability, chemical reactivity, optical polarizability and chemical hardness–softness of a compound [44] (Table 4).

Firstly, in this study, we calculated the HOMO and LUMO orbital energies by using B3LYP method with 6-31G which is implemented in Gaussian 09 package [45,56]. All other calculations were performed using the results with some assumptions. The higher values of EHOMO indicate an increase for the electron donor and this means a better inhibitory activity with increasing adsorption of the inhibitor on a metal surface, whereas ELUMO indicates the ability to accept electron of the molecule. The adsorption ability of the inhibitor to the metal surface increases with increasing of EHOMO and decreasing of ELUMO. The HOMO and LUMO orbital energies of the P2 inhibitors were performed and were shown in Table 5 and Figure 6. High ionization energy (> 6 eV) indicates high stability of P2 inhibitor [47], the number of electrons transferred (ΔN), dipole moment, Ionization potential, electron affinity, electronegativity, hardness, Softness and total energy were also calculated and tabulated in Table 5.

Table 5: Quantum chemical parameters for P2 obtained in gas and aqueous phase with the DFT at the B3LYP/6-31G level.

Parameters	Gas phase	Aqueous phase
Total Energy *TE* (eV)	-17942.6	-17943.2
E_{HOMO} (eV)	-6.6588	-6.4284
E_{LUMO} (eV)	-2.9044	-2.9958
Gap *ΔE* (eV)	3.7544	3.4325
Dipole moment *μ* (Debye)	3.4418	4.6193
Ionization potential *I* (eV)	6.6588	6.4284
Electron affinity *A*	2.9044	2.9958
Electronegativity *χ*	4.7816	4.7121
Hardness *η*	1.8772	1.7163
Electrophilicity index *ω*	6.0898	6.4686
Softness *σ*	0.5327	0.5827
Fractions of electron transferred *ΔN*	0.5909	0.6665

The value of ΔN (number of electrons transferred) show that the inhibition efficiency resulting from electron donation agrees with Lukovit's study [48]. If ΔN<3.6, the inhibition efficiency increases by increasing electron donation ability of these inhibitors to donate electrons to the metal surface [49,50]. Pertinent valence and dihedral angles, in degree, of the studied inhibitor calculated at B3LYP/6-31G(d,p) in gas and aqueous phases are given in the Table 5.

The geometry of P2 in gas and aqueous phase (Figure 6) were fully optimized using DFT based on Beck's three parameters exchange functional and Lee–Yang–Parr non-local correlation functional (B3LYP) [51] and the 6–31G. The optimized structure shows that the molecule P2 has a non-planar structure. The HOMO and LUMO electrons density distributions of P2 are given in Table 6.
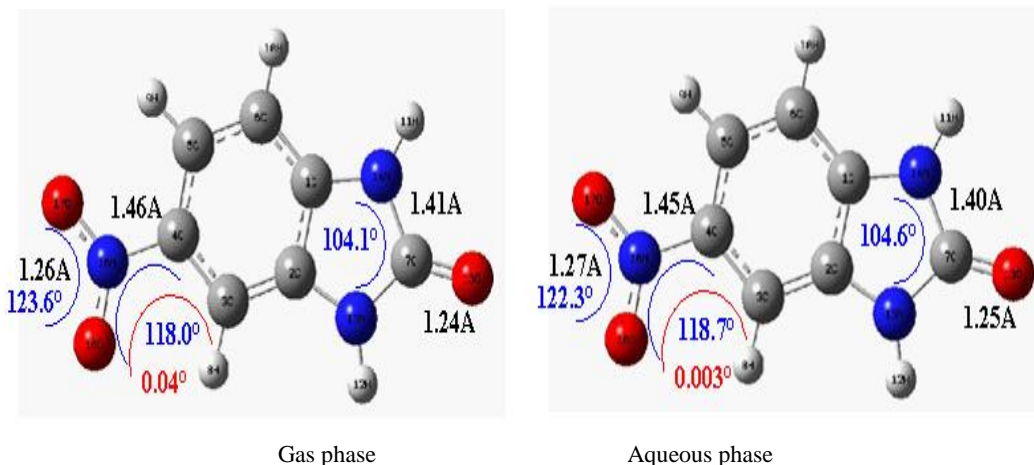
Gas phase   Aqueous phase

Figure 6: Optimized molecular structures and selected dihedral angles (red), angles (blue) and bond lengths (black) of the studied inhibitors calculated in gaseous and aqueous phases using the DFT at the B3LYP/6-31G level.

As we know, frontier orbital theory is useful in predicting the adsorption centers of the inhibitors responsible for the interaction with surface metal atoms. Table 6 shows the HOMO and LUMO orbital contributions for the neutral studied inhibitor. The HOMO densities were concentrated on isotone ring (Figure 7).

	Gas	Aqueous
HOMO		
LUMO		

Figure 7: The HOMO and the LUMO electrons density distributions of P2 in gas and aqueous phase computed at B3LYP/6-31G level for neutral forms.

CONCLUSION

The corrosion inhibition of compound P2 for mild steel in 1 M HCl was evaluated using chemical and electrochemical measurements. The obtained results showed that this inhibitor has good inhibition efficiency, which increases with the inhibitor concentration. The value of adsorption equilibrium constant (K) suggested that this inhibitor is strongly adsorbed on the mild steel surface according to Langmuir adsorption isotherm. Potentiodynamic polarization study shows that studied inhibitor is a mixed type inhibitor.

REFERENCES

[1]   El-Taib, HF., *Corros Sci*, **1980**. 20: 887-896.

[2]   Al-Abdullah, M.M., *Corrosion*, **1991**. 22: 150-154.

[3]   Abdennaby, A.M.S., *Corros Sci*, **1996**. 38: 1791-1800.

[4]   Mernari B., *Corros Sci*, **1998**, 40: 391-399.

[5]   Lukovits, I., *Corrosion*, **1995**. 51: 201-205.

[6]   Bentiss, F., *J Heterocyclic Chem*, **1999**. 36:149-152.

[7]   Bentiss, F., *Corros Sci*, **1999**. 41: 789.

[8]   Chetouani, A., *Der Pharma Chemica*, **2011**. 3: 307-316.

[9]   Gupta, SK.*, J Pharm Sci & Res*, **2010**. 2(4): 228-231.

[10] Vijaya, B., *Asian J Research Chem*, **2009**. 2(2): 162-167.

[11] Jadhav, SB., *Indian J Heterocyclic Chem,* **2009**. 18: 319-320.

[12] Leonard, JT., *Asian J Chem*, **2007**. 19(1):116-120.

[13] Sreena, K., *HYGEIA*, **2009**. 1(1): 21-22.

[14] Simone, B., *ARKIVOC*, **2009**. 3: 225-250.

[15] Ashish Kumar, T., *Indian J Chem*, **2006**. 45: 489-493.

[16] Starcevic, K., *Bioorg Med Chem*, **2007**. 15(13): 4419-4426.

[17] Avci, G., *Colloids Surf A*, **2008**. 317: 730-736.

[18] Noor, E.A., *Mater. Chem. Phys*, **2008**. 110: 145-154.

[19] Gece, G., *Corros Sci*, **2010**. 52: 3304-3308.

[20] Radilla, J., *Electrochim Acta*. **2013**. 112: 577-586.

[21] Arslan, T., *Corros Sci*, **2009**. 51: 35-47.

[22] Pearson, R.G.*, Inorg* Chem, **1988**. 27: 734-740.

[23] Sastri, VS., *Corrosion,* **1997**. 53: 617-622.

[24] Pearson, R.G., *Inorg Chem*, **1988**. 27: 734.

[25] Abd-El-Nabey, A., *Corrosion,* **1996**. 52: 671.

[26] Udhayakala, P., *Journal of Chemical, Biological and Physical Sciences A,* **2012**, 2(3): 1151-1165.

[27] Elmsellem, H., *J Chem Pharm Res*, **2014.** 6: 1216.

[28] Elmsellem, H., *Phys Chem News*, **2013**. 70: 84.

[29] Elmsellem, H., *Der Pharma Chemica*, **2016.** 8(1): 248-256.

[30] Aouniti, A., Journal of Taibah University for Science, **2015**.

[31] Elmsellem, H., *Der Pharma Chemica*, **2015**. 7(10): 237-245.

[32] El Ouadi, Y., *Der Pharma Chemica*, **2016**. 8(1): 365-373.

[33] Elmsellem, H., *Russian, Journal of Applied Chemistry*, **2014**. 87(6): 744-753.

[34] Elmsellem, H., *Int J Electrochem Sci,* **2014**. 9: 5328.

[35] Elmsellem, H., *Protection of Metals, and Physical Chemistry of Surfaces*, **2015**. 51(5): 873.

[36] Elmsellem, H., *Portugaliae Electrochimica Acta*, **2014.** 2: 77.

[37] Elmsellem, H., *Maghr J Pure & Appl Sci*, **2015**. 1: 1-10.

[38] Elmsellem, H., *Der Pharma Chemica*, **2015**. 7(7): 353-364.

[39] Elmsellem, H., *Mor J Chem*, **2014**. 2 (1): 1-9.

[40] Sikine M., *J Mater Environ Sci*, **2016**. 7 (4): 1386-1395.

[41] Hjouji, M., *J Mater Environ Sci*, **2016**. 7(4): 1425-1435.

[42] Chakib, I., *J Mater Environ Sci*, **2016**. 7(6): 1866-1881.

[43] Filali Baba, Y., *J Mater Environ Sci,* **2016**. 7 (7): 2424-2434.

[44] Govindarajan, M., *Spectrochim Acta Part a Mol Biomol Spectrosc,* **2012**. 85: 251-60.

[45] Becke, A.D., *J Chem Phys,* **1993**. 98: 1372.

[46] Filali Baba, Y., *Der Pharma Chemica*, **2016**. 8(4):159-169.

[47] Sebbar, N.K., *J Mater Environ Sci,* **2015**. 6 (11): 3034-3044.

[48] Lukovits, I., *Corrosion*, **2001.** 57: 3-7.

[49] Lahmidi, S., *J Mater Environ Sci,* **2017**. 8(1): 225-237.

[50] Elmsellem, H., *Der Pharma Chemica*, **2016**. 8(1): 248-256.

[51] Sikine, M., *J Mater Environ Sci,* **2017**. 8(1): 116-133.